

Hard Disks in Narrow Channels

Ch. Forster

*Institut für Experimentalphysik, Universität Wien, Boltzmannngasse 5, A-1090 Wien,
Austria*

E-mail: tina@ap.univie.ac.at

D. Mukamel

*Department of physics of complex systems, Weizmann Institute of Science
Rehovot, Israel 76100*

E-mail: david.mukamel@weizmann.ac.il

H. A. Posch

*Institut für Experimentalphysik, Universität Wien, Boltzmannngasse 5, A-1090 Wien,
Austria*

E-mail: posch@ls.exp.univie.ac.at

(November 21, 2018)

The thermodynamic and dynamical behavior of a gas of hard disks in a narrow channel is studied theoretically and numerically. Using a virial expansion we find that the pressure and collision frequency curves exhibit a singularity at a channel width corresponding to twice the disk diameter. As expected, the maximum Lyapunov exponent is also found to display a similar behavior. At high density these curves are dominated by solid-like configurations which are different from the bulk ones, due to the channel boundary conditions.

I. INTRODUCTION

The thermodynamic behavior of hard-disk systems has been a subject of considerable interest in recent years [1]. In particular, the freezing transition taking place in these systems has been analysed by computer simulations for cases where the aspect ratio of the simulation box is close to one. Furthermore, the dynamical stability of such systems has been studied in detail and Lyapunov spectra have been computed [2,3]. The maximum Lyapunov exponent was found to exhibit a maximum in the density regime characteristic for the fluid-to-solid transition [4]. In a restricted geometry, such as a narrow channel, one expects other interesting features to emerge when the width of the channel becomes comparable to the disk's size. Studying narrow channels also enables one to examine long-wavelength perturbed states associated with the small positive Lyapunov exponents found in the tangent-space dynamics of hard-disk and hard-sphere systems [2,3]. This provided the motivation for us to re-investigate the thermodynamic and dynamical properties of a hard-disk gas in a narrow channel.

It is found that for narrow channels the pressure exhibits a singularity at a channel width equal to twice the diameter of the disks. Narrower channels do not allow particles to pass each other. At the same width a singularity is also observed for the collision frequency. In addition, the maximum Lyapunov exponent and the Kolmogorov-Sinai entropy display a non-trivial dependence on the channel width in this regime.

The model we study consists of N hard disks in a two-dimensional box with side lengths L_x, L_y and aspect ratio $A = L_y/L_x$. We vary the width of the box, keeping the volume $V = L_x L_y$ and the particle density $\rho = N/V$ constant. Very small aspect ratios $A \ll 1$ are considered, for which the box resembles a narrow channel. For most of our work we use *periodic* boundary conditions in both directions. Exact thermodynamic properties are known for extremely narrow channels in this case $L_y < \sqrt{3}\sigma$ [5,6]. Recently, the transport properties of two particles in a square periodic box, $A = 1$, have been studied by computer simulation [7]. The case of two particles with *reflecting* boundary conditions in both directions has also received attention, both by molecular dynamics [8] and analytical approaches [9]. It was found that for certain aspect ratios the compressibility becomes negative. We find analogous results also for partly-reflecting boundaries, which are reflecting for the walls parallel to the long direction of the box, x , and periodic for the walls parallel to y .

Throughout, reduced units are used for which the disk diameter σ , the particle mass m and the kinetic energy per particle, K/N , are unity. There is no potential energy in this case, and the total energy E is identical to the kinetic energy K . As a consequence, the temperature T is just an irrelevant parameter and is fixed to unity. Also Boltzmann's constant k is taken unity.

The paper is organized as follows. In Section II we consider the low-density limit. In Section II A we present an analytical derivation of the pressure and show that the singularity taking place at $L_y = 2$ already exists in this limit. In addition, we obtain an analytical expression for the collision frequency which shows a behavior very similar to that of the pressure. Results of numerical simulations of these quantities and of the Lyapunov spectra are presented in Section II B. A numerical study of the high-density case is presented in Section III. Full Lyapunov spectra for periodic systems with periodic boundaries are discussed in Section IV. We close with a brief discussion of the results in Section V.

II. LOW-DENSITY LIMIT FOR SYSTEMS WITH PERIODIC BOUNDARIES

A. Virial approach to the equation of state and collision frequency

The pressure in the low-density limit is obtained by the leading terms in the virial expansion as applied to the narrow-channel geometry. Let $q(L_y)$ be the excluded volume of a single disk in the channel. The phase-space volume associated with placing N disks in the channel is given by

$$\Omega(N) = V(V - q) \dots (V - (N - 1)q), \quad (1)$$

which, to leading order in the density, is reduced to

$$\Omega(N) \simeq V^N \left(1 - \frac{N(N - 1)q}{2V} \right) \simeq V^N \left(1 - \frac{q}{2v} \right)^{N-1}. \quad (2)$$

Here, $v = V/N$ is the specific volume. For low density the specific entropy of the gas is given by

$$s \equiv \frac{S}{N} = k \ln \left(v - \frac{q(L_y)}{2} \right), \quad (3)$$

where k is Boltzmann's constant.

For $L_y > 2$ the excluded area is simply given by the area of a disk of radius 1, namely $q(L_y > 2) = \pi$. To leading order in the density, the pressure P is given by

$$\frac{Pv}{kT} = v \frac{\partial s}{\partial v} \simeq 1 + \frac{\pi}{2v}, \quad (4)$$

and is thus independent of the channel width L_y . This is the expected leading-order expression of the virial expansion of a gas of hard disks.

For $1 < L_y < 2$, however, the excluded area is reduced due to the interference with the disk image resulting from the periodic boundary condition in the y direction (see Fig. 1). Simple geometrical considerations yield

$$q(L_y) = 2\theta + \sin(2\theta), \quad (5)$$

where

$$L_y = 2 \sin(\theta). \quad (6)$$

The excluded volume $q(L_y)$ depends on L_y . Taking the derivative of the entropy with respect to the volume and keeping the aspect ratio $A \equiv L_y/L_x$ constant, one finds to leading order in the density

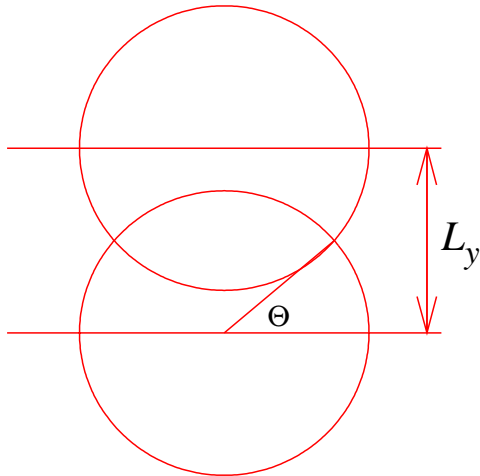


FIG. 1. The excluded area associated with a disk in a channel of width $L_y < 2$ for the case of periodic boundary conditions. The area $q(L_y)$ is given by that of the union of the disk and its translationally-displaced image within the channel.

$$\frac{Pv}{kT} = 1 + \frac{q(L_y)}{2v} - \frac{L_y}{4v} \sqrt{4 - L_y^2}. \quad (7)$$

Note that the pressure curve exhibits a square root singularity as one approaches $L_y = 2$ from below.

The singularity at $L_y = 2$ does not signify a phase transition in the usual sense as it is not a collective phenomenon. In fact, the singularity exists even for finite N and it explicitly shows up in the second term of the virial expansion. This is different from the usual liquid-solid transition in the bulk, which is obtained only after summing over all orders of that expansion. The singularity in the narrow channel is a consequence of the fact that the available volume for the disks is a singular function of the control parameter L_y at $L_y = 2$. Higher order terms in the virial expansion are expected to exhibit a singularity at other integer channel widths, $L_y = 3, 4, \dots$. Thus singularities in the pressure are expected to show up at these widths at higher densities.

We now turn to the evaluation of the collision frequency ν_2 . The virial expression for the pressure, appropriately modified for two-dimensional hard disks, is given by [10]

$$\frac{PV}{NkT} = 1 + \frac{1}{2NkT\tau} \sum_c \mathbf{r}_c \cdot \mathbf{v}_c, \quad (8)$$

where the sum is over all collisions taking place during the time interval τ . Here, the relative position vector of two colliding particles i and j at the time of the

collision, $\mathbf{r}_c \equiv \mathbf{r}_i - \mathbf{r}_j$, satisfies $|\mathbf{r}_c| = \sigma$, and $\mathbf{v}_c \equiv \mathbf{v}_i - \mathbf{v}_j$ is the corresponding relative pre-collision velocity. This may be written as

$$\frac{PV}{NkT} - 1 = \frac{1}{2kT}\nu_2\Delta p \quad (9)$$

where Δp is the average momentum transfer in a collision. For a large aspect ratio A the collision frequency is given by [11]

$$\nu_2 = 2\pi^{1/2}(kT)^{1/2}(\sigma/v)g(\sigma), \quad (10)$$

where $g(r)$ is the pair distribution function. At contact, $r = \sigma$, and in the low-density limit one has $g(\sigma) = 1$. Combining this result with the Eqs. (4) and (9), one finds for the average momentum transfer

$$\Delta p = (\sqrt{\pi}/2)\sqrt{kT}. \quad (11)$$

This expression may also be derived directly from the Maxwell-Boltzmann velocity distribution. It is expected to hold also for narrow channels. The reason is that in the narrow channel the velocity distribution is still isotropic and is given by the Maxwell-Boltzmann distribution (see Section II B). Therefore, one can use Eq. (11), together with Eq. (9), to obtain the collision frequency for narrow channels:

$$\frac{\nu_2}{\sqrt{kT}} = \frac{4}{\sqrt{\pi}} \left(\frac{Pv}{kT} - 1 \right) \quad (12)$$

This expression is valid both below and above $L_y = 2$.

It is expected that in such a highly anisotropic system the pressure tensor is not isotropic. In the low-density limit one can evaluate the diagonal components of the pressure tensor, P_{xx} and P_{yy} , using again the expression for the entropy in Eq. (3). One finds

$$\begin{aligned} P_{xx} &= L_x \left(\frac{\partial s}{\partial L_x} \right)_{L_y} = \frac{v}{v - (1/2)q(L_y)}, \\ P_{yy} &= L_y \left(\frac{\partial s}{\partial L_y} \right)_{L_x} = \frac{v - (1/2)L_y\sqrt{4 - L_y^2}}{v - (1/2)q}. \end{aligned} \quad (13)$$

Furthermore, one has

$$v \left(\frac{\partial s}{\partial v} \right)_A = \frac{1}{2}L_x \left(\frac{\partial s}{\partial L_x} \right)_{L_y} + \frac{1}{2}L_y \left(\frac{\partial s}{\partial L_y} \right)_{L_x},$$

and, hence, $P = (P_{xx} + P_{yy})/2$.

It is evident that in the low-density limit the pressure tensor is isotropic for $L_y > 2$. It becomes anisotropic for $L_y < 2$. At higher densities the two pressure-tensor components differ even above $L_y = 2$ (see Section III). The square-root singularity of the total pressure P at $L_y = 2$ originates from P_{yy} . The other component, P_{xx} , exhibits a weaker singularity.

B. Numerical simulations

Here we carry out numerical simulations for the computation of the pressure, the collision frequency and the Lyapunov exponents. The pressure is evaluated from the impulsive version of the virial theorem Eq. (8) [12,13]. The collision frequency of a single particle, ν_2 , is obtained from the total number of collisions per unit time, divided by $N/2$. For the Lyapunov spectrum we use the algorithm outlined in Refs. [4] and [2]. For the *periodic*-boundary case the linear momentum is conserved both in x and y directions, and, as expected, altogether 6 Lyapunov exponents vanish due to the conservation of energy, momentum, center of mass (only in tangent space), and the regularity of the dynamics in the phase-flow direction. For the *partly-reflecting* boundary case only four of the exponents vanish due to a lack of momentum and center-of-mass conservation in the y direction. The Kolmogorov-Sinai (KS) entropy, h_{KS} , which measures the rate of information gain on the initial conditions due to the time-reversible dynamics, is given by the sum of the positive exponents [14]. Since its dependence on the channel width is qualitatively similar to that of the maximum Lyapunov exponent λ_1 we concentrate on the latter in the following.

In Figure 2 we compare the theoretical curves for the pressure and collision frequency, Eqs. (4), (7) and (12), with the numerical results. In this low-density regime an excellent agreement is obtained. Also shown in this figures is the channel-width dependence of the maximum Lyapunov exponent. It shows a shoulder at the critical width $L_y = 2$. The tangent-space perturbation associated with λ_1 has been shown to be localized in space [3]. This exponent is closely connected to the collision frequency and, as a consequence, has a similar qualitative behavior. This is particularly pronounced in the high density regime as dealt with in the next section.

In Fig. 3 we compare the theoretical curves for the pressure-tensor components P_{xx} and P_{yy} with computer simulations for a density $\rho = 0.01$ and find excellent agreement. As noted above, it is evident that the square-root singularity of P originates from P_{yy} .

It is interesting to note that in the narrow-channel regime, $L_y < 2$, the velocity distribution is still isotropic and is given by the Maxwell-Boltzmann distribution as is shown in Fig. 4. This supports the use of Eq. (11) for the average momentum transfer at a collision even for $L_y < 2$.

The singular behavior of the pressure is due to a sharp increase of the collision frequency as one approaches $L_y = 2$ from below. As can be seen in Fig. 2 the maximum Lyapunov exponent is reminiscent of this singularity as it is closely related to the collision frequency. At this low density this singularity is not clearly pronounced. However as will be shown below, at high densities the existence of a cusp at $L_y = 2$ is evident. The increase of the collision frequency is due to arresting configurations in which a pair of disks become trapped due to the boundaries.

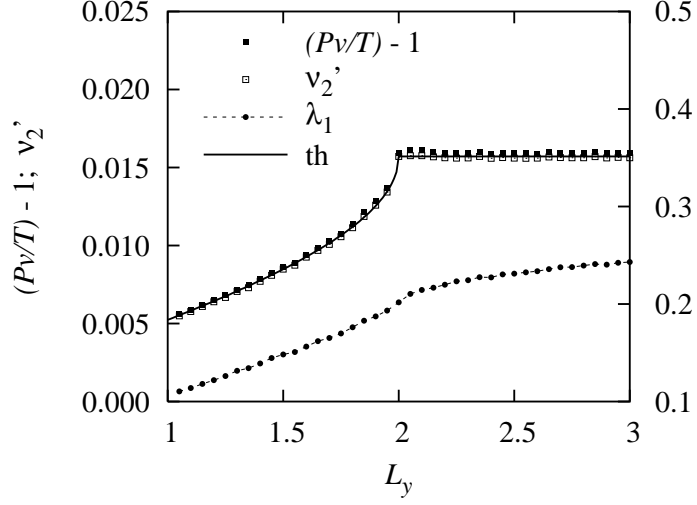


FIG. 2. Theoretical and simulation results for $N = 20$ particles and a density $\rho = 0.01$ for the periodic-boundary case. Shown is the dependence of the maximum Lyapunov exponent λ_1 (right vertical scale), and of the equation of state $(Pv/T) - 1$ (left vertical scale, full squares), and the rescaled single-particle collision frequency $\nu_2' = (\sqrt{\pi}/4)\nu_2$ (left vertical scale, open squares) on the channel width L_y . The full line is computed from Eq. (7).

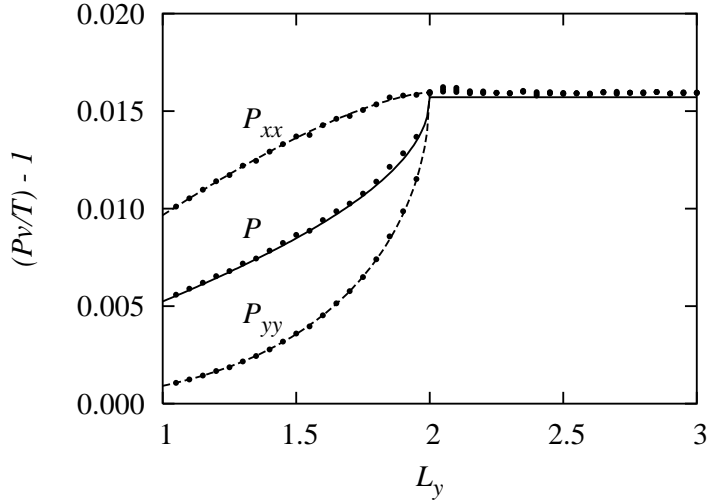


FIG. 3. Comparison of the L_y -dependence of the theoretical curves for $(Pv/T) - 1$, $(P_{xx}v/T) - 1$, and $(P_{yy}v/T) - 1$ (lines) with numerical simulations (points) for a system with 20 disks at a density $\rho = 0.01$.

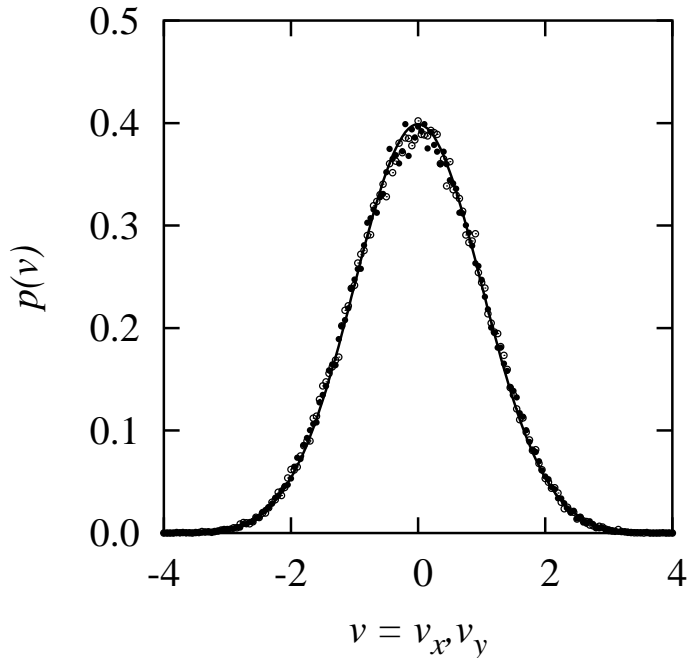


FIG. 4. Distribution of the x and y components of the velocity (open and full circles) for a box of width $L_y = 1.8$. The full line corresponds to a Gaussian distribution.

III. HIGH DENSITY REGIME

For hard-disk systems at high density one has to rely only on numerical simulations. In Fig. 5 we present the pressure, the collision frequency and the maximum Lyapunov exponent as a function of L_y at a density $\rho = 0.4$. It is observed that the singularity taking place at $L_y = 2$ persists at high density in all three curves. According to Eq. (12) the curves for the collision frequency and for $Pv/T - 1$ are proportional with a proportionality constant independent of the density. This is evidently confirmed in Fig. 5. For the special case of only $N = 2$ particles in a square periodic box, the singularity at $L_y = 2$ appears at the critical density $\rho_c = 0.5$ and has recently been observed [7].

When the density is increased beyond 0.5, a broad peak emerges at some $L_y < 2$ in the curves for the pressure and the maximum Lyapunov exponent. This is demonstrated in Fig. 6. This feature is attributed to the pronounced short-range crystalline-like order which is induced by the narrow-channel boundary conditions. Note that this order is not the natural triangular lattice of the system in the bulk. A typical microscopic configuration corresponding to this structure for a density 0.9 and $L_y = 1.5$ is shown in Fig. 7. The particles are arrested and cannot travel across the system, which has been referred to as the localized regime [7].

We have computed also the two pressure-tensor components P_{xx} and P_{yy} for

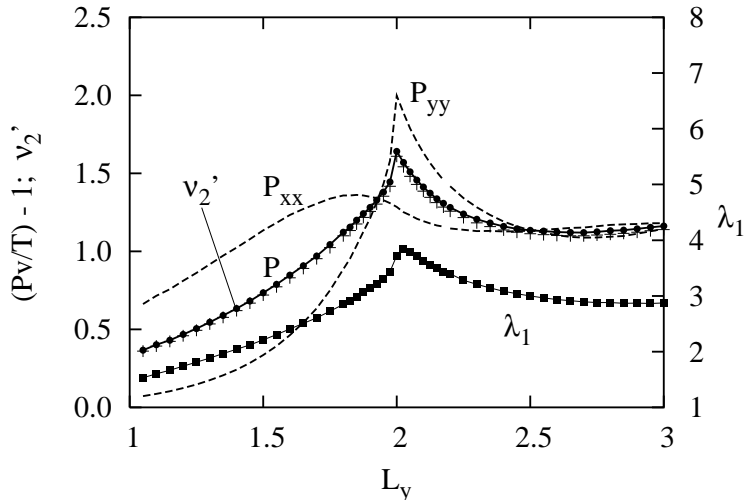


FIG. 5. Simulation results for $N = 20$ particles and a density $N/V = 0.4$ for the periodic-boundary case. Shown is the dependence of the maximum Lyapunov exponent, λ_1 (right vertical scale), of the equation-of-state function $(Pv/kT) - 1$ (full circles with label P , left vertical scale), and of the rescaled single-particle collision frequency, $\nu'_2 = [(\pi/kT)^{1/2}/4] \nu_2$ (crosses, left vertical scale) on the channel width L_y . ν'_2 agrees well with P . The dashed curves labelled P_{xx} and P_{yy} give the contributions $(P_{xx}v/kT) - 1$ and $(P_{yy}v/kT) - 1$ of the respective pressure-tensor components.

a system with a density $\rho = 0.8$. As can be seen in Fig. 8, the two components are significantly different both above and below $L_y = 2$. The singularity of the pressure at $L_y = 2$ is evidently caused by P_{yy} , as is also the case for low densities.

All the examples so far are for the case of periodic boundaries in both the x and y directions. A qualitatively similar result is obtained, if the long sides of the channel are elastically reflective, whereas the short sides remain periodic. This is demonstrated in Fig. 9 for $N = 100$ particles at a density of $N/V = 0.4$, where P , λ_1 and ν are shown as a function of the box width L_y . The maxima are not as sharp as in Fig. 5 for the periodic case, but are as pronounced.

In order to get some insight into the dynamics of such systems it is usually useful to study the diffusion coefficient. It is well known that this coefficient does not exist in two-dimensional systems in the thermodynamic limit [15]. However, it is possible to compute the mean-squared displacement for a *finite* system and to extract effective diffusion constants D_x and D_y in x and y directions, respectively. They are obtained from fits to the linear growth of $\langle \Delta x^2 \rangle$ and $\langle \Delta y^2 \rangle$ for times $t > 40$. The results for a density $\rho = 0.8$ are shown in Figure 10. As expected D_x vanishes for $L_y < 2$, while D_y is non-zero. In fact, D_y increases with L_y approaching unity as a result of the periodic-boundary restrictions disfavoring momentum exchange in the y direction. Another interesting feature of Fig. 10

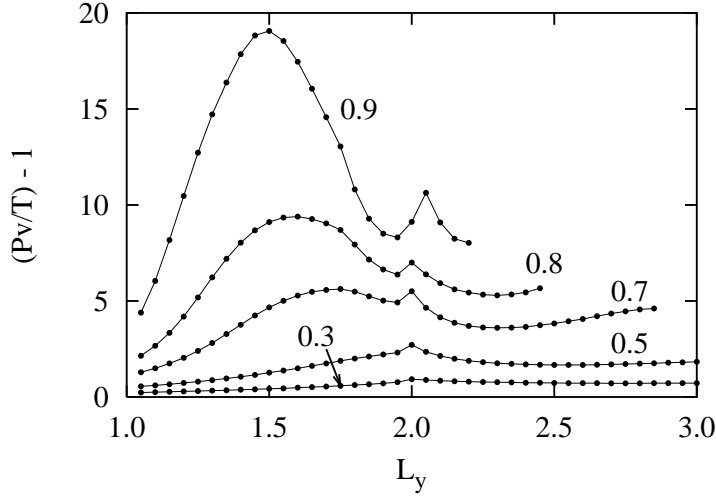


FIG. 6. L_y dependence of the pressure for various densities as indicated by the labels.

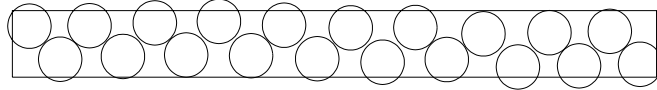


FIG. 7. A typical microscopic configuration for a density $\rho = 0.9$ and a channel width $L_y = 1.5$. It resembles the closest-dense packing consistent with the periodic boundaries. It minimizes the mean free path and, hence, maximizes the collision frequency and the pressure.

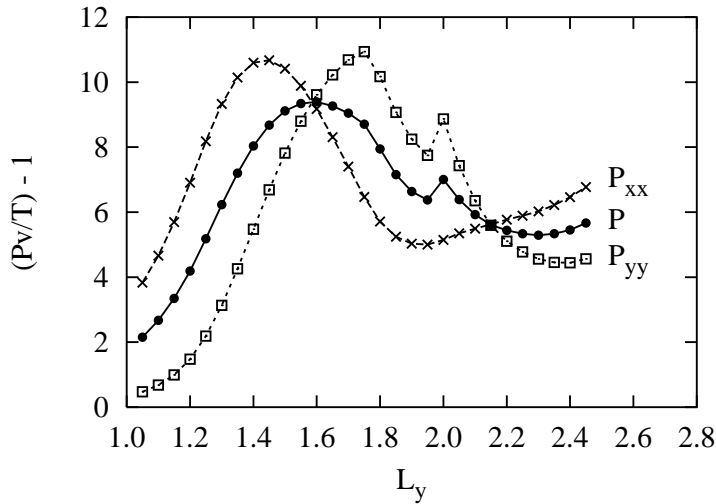


FIG. 8. Simulation results for the pressure curves $(Pv/T) - 1$, $(P_{xx}v/T) - 1$, and $(P_{yy}v/T) - 1$ as a function of the channel width L_y . The system consists of $N = 20$ particles at a density $\rho = 0.8$.

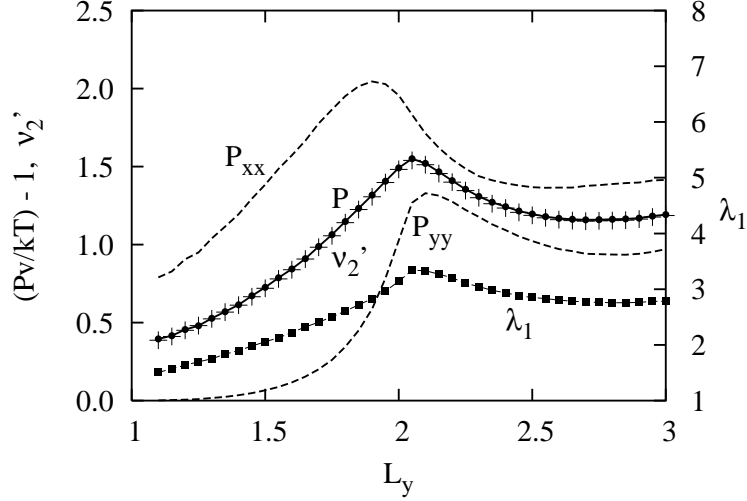


FIG. 9. Simulation results for $N = 20$ particles and a density $N/V = 0.4$ in a rectangular box with partly-reflecting boundaries (see the main text). Shown is the dependence of the maximum Lyapunov exponent, λ_1 (right vertical scale), of the equation-of-state function $(Pv/kT) - 1$ (full circles with label P , left vertical scale), and of the rescaled single-particle collision frequency, $\nu_2' = [(\pi/kT)^{1/2}/4] \nu_2$ (crosses, left vertical scale) on the channel width L_y . ν_2' agrees well with P . The dashed curves labelled P_{xx} and P_{yy} give the contributions $(P_{xx}v/kT) - 1$ and $(P_{yy}v/kT) - 1$ of the respective pressure-tensor components.

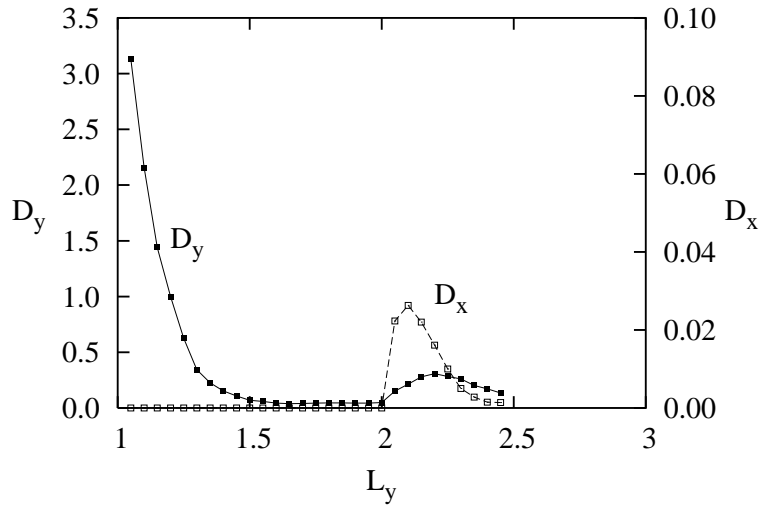


FIG. 10. Effective diffusion constants (see the main text) in x and y directions for disks in a narrow-channel with periodic boundaries at a density $\rho = 0.8$.

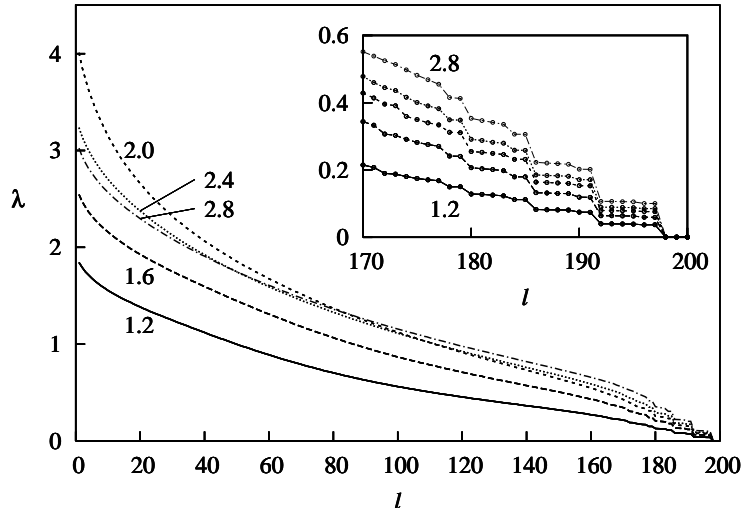


FIG. 11. Positive branches of Lyapunov spectra for 100-disk systems with *periodic* boundaries. The box width, L_y , is indicated by the labels. The density, $\rho = 0.4$, and the Volume, $L_x L_y$, are fixed. The Lyapunov exponents are defined only for integer values of the index l . In the inset the regime supporting Lyapunov modes is magnified. There, L_y increases from 1.2 (bottom) to 2.8 (top) in steps of 0.4. For details we refer to the main text.

is the vanishing of D_x and D_y for $L_y > 2.7$. This is due solid-like triangular configurations characteristic of the bulk at this high density.

IV. SOME REMARKS ON LYAPUNOV SPECTRA

In Fig. 11 we plot the Lyapunov spectra for a 100-disk system in a narrow periodic box. All spectra are for a density $\rho = 0.4$, which corresponds to a fluid. Since the volume, $L_x L_y$, is fixed, an increase of the channel width L_y , varied in the figure in steps of 0.4, decreases L_x accordingly. L_y is indicated by the labels. Each spectrum consists of $4N$ Lyapunov exponents, of which only the positive branch, $\{\lambda_l \geq 0; l = 1, 2, \dots, 2N\}$, is shown. The spectra are only defined for integer values of the index, l , which labels the exponents according to size. The lines are only drawn for clarity. According to the equilibrium formulation of the conjugate-pairing rule, the negative branch of the spectra, $\{\lambda_l \geq 0; l = 2N + 1, \dots, 4N\}$, is the mirror image of the positive branch [16].

The inset of Fig. 11 provides a magnified view of the small exponents. They turn out to be degenerate, which gives rise to a step-like appearance of the spectra [4]. The tangent-space perturbations associated with these exponents are collective, wave-like fields defined over the simulation box, and are referred to as

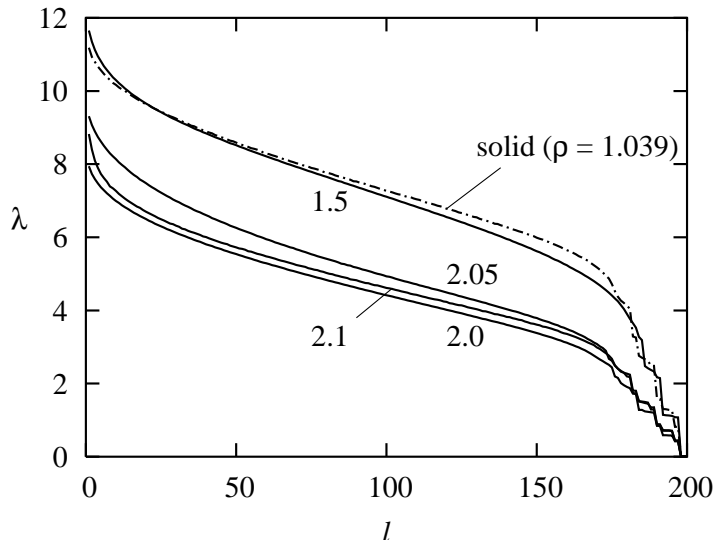


FIG. 12. The Lyapunov spectra plotted by the smooth lines are for 100-disk systems with periodic boundaries, where the density, $\rho = 0.9$, and the volume, $L_x L_y$, are fixed. The resulting box widths, L_y , are indicated by the labels. The dash-dotted curve labeled “solid” is for 100 disks in a periodic channel with an aspect ratio $L_y/L_x = \sqrt{3}/(N/2)$ required for a triangular lattice. The density ρ is also given. For details we refer to the main text. Only the positive branches of the spectra are shown.

Lyapunov modes [2,3,17]. The multiplicity is determined by the intrinsic symmetries of the Hamiltonian and the boundary conditions, which give rise to the conserved quantities, energy and momentum. A complete classification in terms of transverse (T), longitudinal (L), and momentum (P) modes is given in Ref. [20]. Theoretical attempts have been made to interpret the modes in terms of fluctuating hydrodynamics [21–25].

We observe that a particular exponent, say the smallest positive, increases with L_y and, hence, with the wave number, $k = 2\pi/L_x = 2\pi L_y/V$, belonging to this mode. This is referred to as a “dispersion relation” [2,3]. Thus, λ_{2N-3} increases monotonously with L_y . However, as Fig. 11 shows, this proportionality does not hold for the large exponents. There is a crossover of the spectra reversing the sequence of λ near $L_y = 2$. This is mainly a consequence of the collision frequency. The perturbations for the large exponents are found to be localized in space with only a small fraction of the particles contributing to the large exponents at any instant of time. The active zone moves around in space, restoring homogeneity on average.

The smooth lines in Fig. 12 show Lyapunov spectra for analogous 100-disk systems for a density $\rho = 0.9$, where the channel width is indicated by the la-

bels. The case $L_y = 1.5$ corresponds to the arrested structure of Fig. 7 and is of particular interest. In Fig. 12 we compare it with the dash-dotted spectrum of 100 disks in a periodic channel with an aspect ratio $L_y/L_x = \sqrt{3}/(N/2)$. For $L_y = 1.8258$ and $N = 100$, the density is $\rho = 1.039$, and the particles form a triangular lattice characteristic of a solid in the bulk. Although the nearest neighbor separations and, hence, the collision frequencies, are nearly the same for both systems, the Lyapunov spectra are distinctly different. The maximum exponent, λ_1 , for the arrested structure is significantly larger than for the triangular system, whereas the behavior of the smaller exponents is just the reverse. This example demonstrates that the Lyapunov spectra are sensitive to structural details and are potentially a useful tool. But it is fair to say that no theory exists at present to interpret such spectra in full detail.

V. DISCUSSION

In this work the thermodynamic and dynamical behaviour of hard disks in a narrow channel is analysed using analytical and numerical approaches. The main results are for periodic boundary conditions in both x and y directions. Related studies of reflecting boundaries parallel to the channel axis reveal that similar features exist there as well. It is found that the pressure, collision frequency, maximum Lyapunov exponent, and Kolmogorov-Sinai entropy curves exhibit a singularity for a channel width equal to twice the disk diameter. For low densities this singularity for P and ν_2 is well understood by a virial expansion as it already shows up in the second virial coefficient. The singularity is not the result of a collective behavior and, in fact, is present for systems with a finite number of particles. Thus, it is not a genuine phase transition. It is rather a result of a rapid change in the available phase space taking place close to $L_y = 2$. Similar but less pronounced singularities are expected to show up at $L_y = 3$ and larger integers at higher virial coefficients.

The singularity for the maximum exponent and for the KS-entropy is most pronounced for higher densities. This is a consequence of the fact that these quantities are closely related to the collision frequency [11]. It has been established that in bulk systems these quantities exhibit a maximum at a phase transition [18,19]. The maximum Lyapunov exponent is a measure of the fastest dynamical events taking place in a system which are localized processes in space [3]. Thus, its behavior near the transition point is not related to a diverging length scale at the transition. Whereas in an ordinary phase transition in the bulk the enhanced collision frequency - and, thus, of λ_1 - is due to the emergence of a new structure, here it is a consequence of the constraints imposed by the boundaries.

We expect the singularity found for $L_y = 2$ to be present also for soft disks. In this case, however, the singularity is likely to be weaker than the square-root singularity found in the pressure curve of hard disks. Similar features found in

the present study should be present in three-dimensional channels as well. It would be of interest to study these problems in more detail.

ACKNOWLEDGMENTS

We thank the Austrian Science Foundation (FWF), Grant P15348-PHY, and the Israel Science Foundation for support. We also acknowledge the Einstein Center and the Österreichische Gesellschaft der Freunde des Weizmann Institute of Science for support during mutual visits.

-
- [1] T. M. Truskett, S. Torquato, S. Sastry, P. G. Debenedetti, and F. H. Stillinger, *Phys. Rev. E* **58**, 3083 (1998).
 - [2] H. A. Posch and R. Hirschl, p. 269, in *Hard Ball Systems and the Lorenz Gas*, edited by D. Szasz, *Encyclopedia of the mathematical sciences* **101**, Springer Verlag, Berlin (2000).
 - [3] Ch. Forster, R. Hirschl, H. A. Posch, and Wm. G. Hoover, *Physica D*, **187**, 281 (2004).
 - [4] Ch. Dellago, H.A. Posch, and W.G.Hoover, *Phys. Rev. E* **53**, 1485 - 1501 (1996).
 - [5] K. W. Wojciechowski, P.Pieranski, and J. Malecki, *J. Chem. Phys.* **76**, 6170 (1982).
 - [6] K. W. Wojciechowski, P.Pieranski, and J. Malecki, *J. Phys. A: Math. Gen.***16**, 2197 (1983).
 - [7] S. Viscardy and P. Gaspard, *Phys. Rev. E* **68**, 041204 (2003).
 - [8] A. Awazu, *Phys. Rev. E* **63**, 032102 (2001).
 - [9] T. Munakata and G. Hu, *Phys. Rev. E* **65**, 066104 (2002).
 - [10] W. G. Hoover and B. J. Alder, *J. Chem. Phys.* **46**, 686 (1967).
 - [11] R. van Zon, H. van Beijeren, and J. R. Dorfman, p. 321, in *Hard Ball Systems and the Lorenz Gas*, edited by D. Szasz, *Encyclopedia of the mathematical sciences* **101**, Springer Verlag, Berlin (2000).
 - [12] D. C. Rapaport, *The Art of Molecular Dynamics Simulation*, Cambridge University Press, 2001, page 296.
 - [13] M. P. Allen and D. J. Tildesley, *Computer Simulation of Liquids*, Oxford University Press, Oxford (1991).
 - [14] V. I. Oseledec, *Trans. Moskow Math. Soc.* **19**, 197 (1968).
 - [15] B. J. Alder and T. E. Wainwright, *Phys. Rev. A* **1**, 18 (1970).
 - [16] C. P. Dettmann and G. P. Morriss, *Phys. Rev. E* **53**, R5541 (1996).
 - [17] Ch. Forster and H. A. Posch, *Heareus Summer School Proceedings* (2003).
 - [18] H.A. Posch, W.G. Hoover and B.L. Holian, *Ber. d. Bunsenges. f. Phys. Chem.* **94**, 250 - 256 (1990).
 - [19] Ch. Dellago and H. A. Posch, *Physica A*, **237**, 95 - 112 (1997).

- [20] E. Zabey, J.-P. Eckmann, Ch. Forster, and H. A. Posch, in preparation (2004).
- [21] J.-P. Eckmann and O. Gat, *J. Stat. Phys.* **98**, 775 (2000).
- [22] S. McNamara and M. Mareschal, *Phys. Rev. E* **64**, 051103 (2001)
- [23] M. Mareschal and S. McNamara, *Physica D* **187**, 311 (2004).
- [24] T. Taniguchi, C. P. Dettmann, and G. C. Morriss, *J. Stat. Phys.* **109**, 747 (2002).
- [25] A. de Wijn and H. van Beijeren, submitted to *Phys. Rev. E* (2004).